

The effect of upstream turbulence and its anisotropy on the efficiency of solar wind – magnetosphere coupling

D. Jankovičová¹, Z. Vörös^{1,2}, and J. Šimkanin³

¹Institute of Atmospheric Physics, Academy of Sciences of the Czech Republic, Prague, Czech Republic

²Institute of Astro- and Particle Physics, University of Innsbruck, Innsbruck, Austria

³Geophysical Institute, Academy of Sciences of the Czech Republic, Prague, Czech Republic

Received: 20 December 2007 – Revised: 17 April 2008 – Accepted: 29 May 2008 – Published: 2 July 2008

Abstract. The importance of space weather and its forecasting is growing as interest in studying geoeffective processes in the Sun – solar wind – magnetosphere – ionosphere coupled system is increasing. This paper introduces the proper selection criteria for solar wind magnetic turbulence events during duskward electric field and southward B_z driven geomagnetic storms. Two measures for the strength of solar wind fluctuations were investigated: the standard deviations of magnetic field components and a proxy for the so-called Shebalin anisotropy angles. These measures were compared to the strength of geomagnetic storms obtained from a SYM-H index time series. We found a weak correlation between standard deviation of interplanetary magnetic field GSM component B_z and SYM-H index, and a strong correlation between Shebalin anisotropy angle and the SYM-H index, which can be the result of an increase of probability of magnetic reconnection in fluctuating magnetic fields.

1 Introduction

The solar wind is a supersonic plasma flow, originating from the Sun, in which coherent structures, waves and turbulence coexist and interact over various spatial and temporal scales. Some of these structures such as shocks, recurrent streams, etc., can be associated with dynamical processes on the Sun. Multi-scale magnetic and plasma fluctuations are mostly driven locally at different heliocentric distances and exhibit power-law spectral scalings and stretched-tailed non-Gaussian occurrence statistics (Burlaga, 1991; Sorriso-Valvo et al., 1999; Vörös et al., 2002; Bruno and Carbone, 2005).

The investigation of the geoeffectiveness of solar wind turbulence represents a complex problem. The upstream pa-

rameters and fluctuations undergo significant changes across the bow shock and in the magnetosheath. Statistical results indicate that the investigation of upstream solar wind input conditions in relation to geomagnetic response is physically relevant. Despite the dynamical and structural complexity of the solar wind, the gross features of solar wind – magnetosphere interactions and magnetospheric responses can be understood in terms of a few physical parameters or derived quantities in this input-output system. The parameters associated with the solar wind driver (input) usually include bulk plasma parameters (e.g. the solar wind speed, density, etc.) and the strength and orientation of the interplanetary magnetic field. The corresponding time-delayed magnetospheric response (output) is usually represented in terms of various geomagnetic indices. Based on both solar wind input parameters and geomagnetic indices, nonlinear input-output filters were proposed (e.g. Vassiliadis et al., 1996). They explained more than 80% of the time-delayed magnetospheric response. Let us mention some known examples, in which coherent structures, waves and turbulence play an important role in the solar wind – magnetosphere coupling processes:

- Magnetic cloud structures or interplanetary shock compressed regions can be associated with intense and long duration negative interplanetary magnetic field GSM component B_z events and enhanced bulk speed (Gonzalez et al., 2002).
- The interplanetary causes of intense geomagnetic storms ($D_{st} < -100$ nT) are supposed to be a consequence of large and negative solar wind B_z events (< -10 nT) with a duration of more than 3 hours associated with interplanetary duskward electric fields $E_y > 5$ mV/m (Gonzalez and Tsurutani, 1987).
- In some cases, large amplitude interplanetary Alfvén wave trains are associated with intense auroral activity e.g. seen in the AE index (Gonzalez et al., 1999).



Correspondence to: D. Jankovičová
(dja@ufa.cas.cz)

- D’Amicis et al. (2007) have shown that Alfvénic turbulence is geoeffective mainly at solar cycle minimum, while during solar maximum convected structures dominated by an excess of magnetic energy play a role.

The inclusion of geomagnetic indices as input parameters indicates that the magnetosphere is not a passive element, but rather the actual magnetospheric conditions are also important for the prediction of its future behaviour (McPherron et al., 1988).

The multiscale non-Gaussian nature of turbulent fluctuations in the solar wind is not fully understood. Magnetic field fluctuations represent “weak” stationary random functions in the first and second order statistics. Sudden jumps in the time series influence the spectral properties of fluctuations and higher order statistical moments (e.g. skewness and kurtosis) show also non-stationary behaviour, often associated with coherent structures and boundaries in the solar wind (Jankovičová et al., 2008). A turbulent effect is more discernible if other geoeffective parameters are “switched off”, which happens e.g. during particular periods of positive interplanetary magnetic field GSM component B_z . Otherwise, turbulence presumably does not have a completely independent role as it can only amplify or weaken the effect of a “switched on” geoeffective parameter, e.g. the duskward electric field. Borovsky and Funsten (2003) found statistically strong correlations between the amplitude of upstream turbulence (constructed from standard deviations of magnetic field components from ISEE-3 and IMP-8 spacecraft) and geomagnetic indices (AE, AL, AU, Kp, ap, PCI and D_{st}) during northward (positive) B_z conditions. In their studies the duskward electric field E_y shows little or no correlation with the geomagnetic response in this case. In contrast, during southward B_z the correlation between E_y and geomagnetic indices increases and the correlation between turbulence amplitude and geomagnetic indices decreases, but remains statistically significant. Their physical interpretation is straightforward: during northward B_z a viscous coupling of the solar wind flow to the magnetosphere is enhanced and therefore the level of turbulence in the solar wind is the key parameter. On the contrary, when magnetic reconnection operates at the magnetopause during southward B_z , the antiparallel orientations of interplanetary and magnetospheric magnetic fields are essential. Borovsky and Funsten (2003) found that the correlation between upstream magnetic fluctuations and the geomagnetic indices AE, AL, AU, Kp, ap, PCI are stronger than its correlation with the D_{st} index.

In this paper we investigate the influence of upstream magnetic field turbulence on geomagnetic SYM-H index associated with southward interplanetary magnetic field GSM component B_z and enhanced duskward electric field component E_y during geomagnetic storms. The SYM-H index is similar to the D_{st} index. Both D_{st} and SYM-H are indices, which measure the intensity of the storm time ring current. The main difference between the 1 min SYM-H and the hourly

D_{st} index is the time resolution and the effects of the solar wind dynamic pressure variations are more clearly seen in the SYM-H than in the hourly D_{st} index (Wanliss and Showalter, 2006).

2 Methods and data description

2.1 Description of storm associated upstream magnetic turbulence

To characterize magnetic turbulence in the solar wind, we use the standard deviation (std) and the so-called Shebalin anisotropy angle (θ). The first measure is estimated in a standard way, the latter needs more explanation.

2.1.1 The anisotropy angle

Shebalin et al. (1983) studied incompressible 2-D MHD anisotropy arising in wave vector space in the presence of a mean magnetic field. They studied the interaction of opposite-traveling wave packets and found that those interactions produce modes with wave vectors preferentially perpendicular to the mean magnetic field. They introduced the anisotropy angle θ

$$\tan^2 \theta = \frac{\langle k_{\perp}^2 \rangle}{\langle k_{\parallel}^2 \rangle}, \quad (1)$$

as a quantitative measure of spectral anisotropy, where k_{\parallel} and k_{\perp} represent wave numbers parallel and perpendicular to the mean magnetic field direction, respectively. In the 3-D case (e.g. Oughton et al., 1998a; Matthaeus et al., 1998), three special cases are relevant: $\theta \approx 54^\circ$ corresponds to isotropic fluctuations; $\theta = 0^\circ$ (if $k_{\perp} = 0$) to purely parallel (slab) fluctuations and $\theta = 90^\circ$ (if $k_{\parallel} = 0$) to fully perpendicular (2-D) fluctuations. On the basis of theoretical arguments and numerical simulations, Oughton et al. (1998a) showed that the anisotropy angle θ , defined in the Fourier space, can be estimated in the timedomain from the ratio of the fluctuating magnetic field δb to the local magnetic field B_0 as

$$\cos^2 \theta = m \left(\frac{\delta b^2}{B_0^2 + \delta b^2} \right) + c, \quad (2)$$

where m and c depend on the turbulence parameters and can be estimated from Fig. 3 in the work of Oughton et al. (1998a) by e.g., a least square fit over intermediate values of $\delta b / \sqrt{B_0^2 + \delta b^2}$ dashed line as $m \approx 0.4$ and $c \approx 0.01$. Oughton et al. (1998b) showed that the approximate relationship is valid only for some intermediate values

$$0.1 \leq \frac{\delta b}{\sqrt{B_0^2 + \delta b^2}} < 1, \quad (3)$$

where the denominator is the total magnetic field strength.

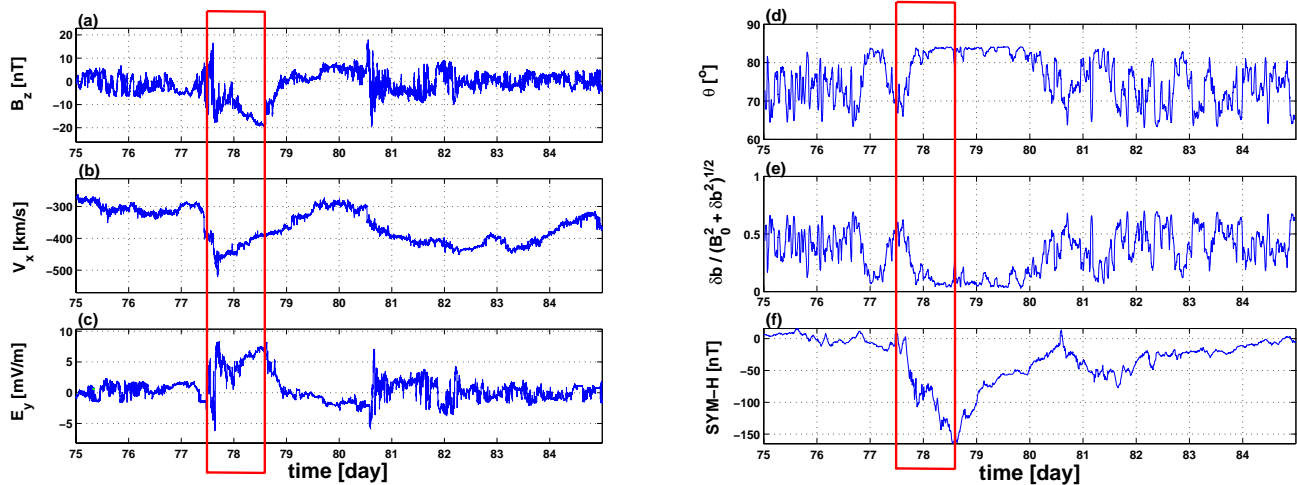


Fig. 1. Geomagnetic storm in March 2001, ACE observations: (a) GSM B_z component of the interplanetary magnetic field; (b) V_x component of bulk speed; (c) the duskward electric field E_y ; (d) the estimated Shebalin anisotropy angle θ ; (e) the ratio of magnetic fluctuations to the local field $\delta b / \sqrt{B_0^2 + \delta b^2}$; (f) SYM-H index.

2.1.2 Sliding window analysis

It is obvious that the geoeffectivity of upstream processes in the solar wind changes over time. Our main goal is to provide a possible quantitative description of non-stationary magnetic fluctuations within sliding overlapping windows. The length of the sliding window W has to be chosen according to the available length of quasi-stationary physical processes. To be able to estimate the spectral properties of fluctuations, W should be as large as possible, but cannot be larger than the lifetime of fluctuations we are interested in. The largest timescale of turbulence in the solar wind is typically less than a day. Below this time scale, power spectra are well-described by a power law slope $\sim 5/3$ and extend over the so-called inertial range, where dissipation is supposed to be negligible and energy cascades toward large wave numbers (small time scales) are governed by nonlinear interactions (e.g. Burlaga and Forman, 2002). On the other hand, the smallest time scale of magnetohydrodynamic turbulence is of the order of some minutes. Therefore, the choice $W=35$ min seems to be reasonable, being well inside the inertial range of turbulence. The window W is time shifted by 16 s along the time series after each calculation step. Within each analyzing window the mean magnetic field, the standard deviation and the Shebalin anisotropy angle are estimated. Fluctuations, δb , in Eqs. (2) and (3) were obtained within each W , as

$$\delta b^2(t, W) = \langle (B_x - \langle B_x \rangle)^2 \rangle + \langle (B_y - \langle B_y \rangle)^2 \rangle + \langle (B_z - \langle B_z \rangle)^2 \rangle. \quad (4)$$

The timescale in this time-domain analysis is represented by W . We note that performing sliding window analysis using slightly different W (different scales) will not change our re-

sults. For proper steady estimations of θ similar values of $\delta b / \sqrt{B_0^2 + \delta b^2}$ were required at least over the length of two windows.

2.2 Solar wind fluctuations vs. magnetospheric response

The existence of possible connections among negative solar wind B_z events (< -10 nT), large interplanetary duskward electric fields E_y (> 5 mV/m), anisotropy of magnetic field fluctuations and magnetic storms is displayed in Fig. 1. The magnetic storm shown in the time series of SYM-H index (Fig. 1f), occurred between days 77 and 84 of 2001. The main phase of the storm (indicated by a red box in Fig. 1) occurred between days 77.5 and 78.6. During that time period B_z is mainly negative and achieves values of -18 nT (Fig. 1a). After a discontinuity on day 77.5, the bulk speed $|V_x|$ component increases up to 500 km/s (Fig. 1b) and the electric field E_y fluctuates around 5 mV/m (Fig. 1c). The estimated Shebalin anisotropy angle and the associated ratio $\delta b / \sqrt{B_0^2 + \delta b^2}$ are depicted in Fig. 1d, e. During the main phase and the beginning of the recovery phase of the storm (between days 78 and 80), $\delta b / \sqrt{B_0^2 + \delta b^2}$ is close to 0.1. Therefore, according to Eq. (3), θ cannot be straightforwardly estimated. Indeed, during that period θ shows almost no variability, but displays saturated values close to 85° . This behaviour is not unique, but repeatedly occurs during some geomagnetic storms. Just before the beginning of the main phase of the storm at day 77.7, $\delta b / \sqrt{B_0^2 + \delta b^2}$ fluctuates around 0.5 and $\theta \sim 70^\circ$ during several sliding window lengths W (Fig. 1d, e). If θ does not fluctuate too much, multi-scale fluctuations occur

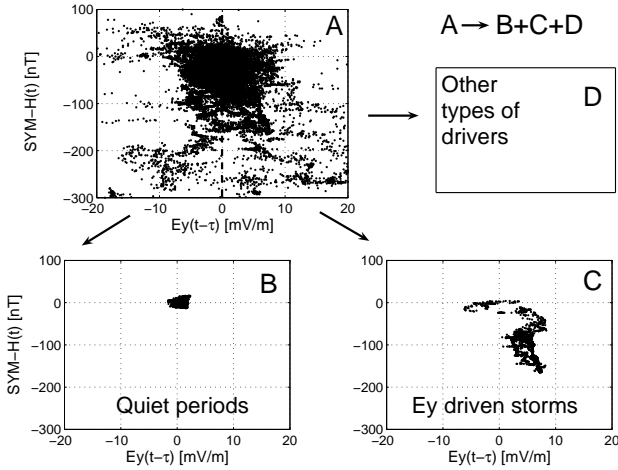


Fig. 2. (A) Scatter plot of SYM-H index vs. duskward electric field for two months of data beginning from March 1, 2001; (B) scatter plot pattern during a quiet interval; (C) scatter plot pattern during an E_y driven geomagnetic storm; (D) other sources. The sources (B), (C), (D), all contribute to the structureless scatter plot in (A).

anyway in B_z and E_y after the shock front visible in V_x on day 77.5. The fluctuations of $\delta b/\sqrt{B_0^2+\delta b^2}$ or θ are larger between days 75 and 77.5 or after day 80, but the proper value of the ratio $\delta b/\sqrt{B_0^2+\delta b^2}$ does not guarantee alone that the estimated θ can be physically related to anisotropy features of cascade turbulence in the presence of mean magnetic field. On the other hand, the simultaneous presence of multiscale magnetic and electric fluctuations during intervals of quasi-steady non-saturated θ indicates that the Shebalin angles might have physical meaning in the relation of solar wind-magnetosphere coupling. We will test this hypothesis considering larger number of events.

3 Results

In order to study the geoeffective processes it is necessary, to find simultaneous interplanetary and geomagnetic data sets. For our analysis we used the time series of 16 s averages of interplanetary magnetic field B_z (GSM) component measurements performed by ACE satellite during years 2000–2002. E_y was constructed from 1 min ACE data for magnetic field and from OMNI combined dataset for bulk speed. As an indicator of magnetospheric response, the SYM-H index with $\Delta\tau=1$ min was chosen. The SYM-H index is ideally regarded as a measure of the magnetospheric ring current intensity.

In order to present clearly our event selection criteria we show how the enhanced level of solar wind-magnetosphere coupling during geomagnetic storms can be represented in $E_y(t-\tau)$ vs. SYM-H(t) scatter plots. τ represents the

time needed to shift the solar wind measurements to Earth using the average solar wind convection velocity, $\langle V_{sw} \rangle$. Fig. 2a shows the scatter plot of $E_y(t-\tau)$ vs. SYM-H(t) for two months of data beginning 1 March 2001. There are no clear structures in it. This fact would be clearly due to the non-stationarity character of both solar wind input and magnetospheric output parameters. Figure 2b, c and d display the contribution of different physical situations to the structureless scatter plot in Fig. 2a. Fluctuations around $E_y(t-\tau)\sim 0$ and SYM-H($t)\sim 0$ occur during quiet periods, during which the solar wind – magnetosphere coupling is negligible (Fig. 2b). A good example of duskward electric field driven storms is represented by the geomagnetic storm in Fig. 1. Figure 2c shows the scatter plot corresponding to the time interval indicated by red box in Fig. 1. The SYM-H index does not change too much when E_y is negative (northward B_z), but in full agreement with Gonzalez and Tsurutani (1987), positive electric fields (southward B_z) evoke a strong geomagnetic response in the form of negative SYM-H reaching a value of -160 nT. Figure 2d implies the possibility of other types of physical processes contributing to the scatter plot in Fig. 2a. These processes include e.g. local processes in the solar wind, internal dynamics of the magnetosphere, the influence of other input parameters on coupling efficiency like density or (e.g. Borovsky and Funsten, 2003). Moreover, the solar wind bulk speed changes in time so that the average convection velocity $\langle V_{sw} \rangle$ and the time shift τ do not characterize well longer time periods. Consequently the characteristic E_y driven patterns (e.g. in Fig. 2c) get smeared or even lost. A practical way to find a proper τ is to compute its approximate value using the convection velocity and systematically changing of τ around mean value in the given interval ($l/\langle V_{sw} \rangle$, where l is the distance between L_1 and Earth) to find as large a coherency in scatter plot pattern in Fig. 2c as possible. τ is not the only one time parameter, which has to be considered in comparison of solar wind input to magnetospheric response. The linear correlation coefficients between solar wind magnetic field fluctuations and the D_{st} index reach the largest values at a time lag of few hours (Borovsky and Funsten, 2003). It happens because the autocorrelation time of solar wind fluctuations is of the order of hours and also because of the gradual build-up of the magnetospheric current systems.

In this paper we estimate the standard deviations of magnetic field components and the Shebalin anisotropy angle (θ) during 0.1 day long time intervals from time shifted solar wind measurements in cases of duskward electric field driven geomagnetic storms. The time intervals 0.1 day long were chosen in order to simultaneously satisfy two conditions: (i) to have enough proper events and (ii) std and θ to have as small errors as possible. If intervals would have been longer than 0.1 day we had had less amount proper intervals, but even std and θ would have been with much less errors. If shorter, we had had more proper intervals, but with std and θ with much greater errors. From this point

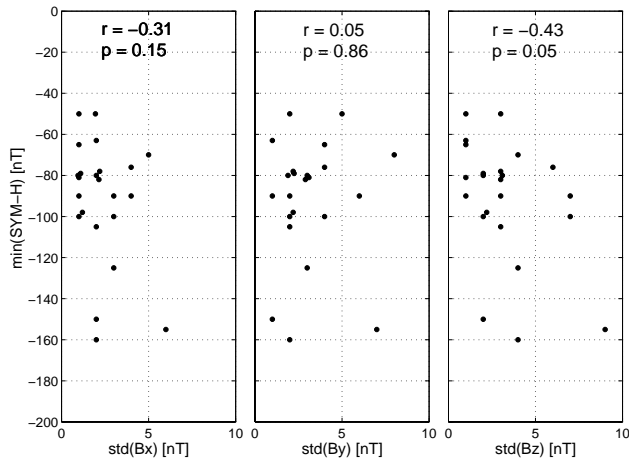


Fig. 3. The time delayed maximum strength of geomagnetic storms, measured by $\min(\text{SYM-H})$, is plotted as a function of standard deviations of interplanetary magnetic field GSM components B_x , B_y , B_z . The correlation coefficients (r) and the corresponding p-values are shown in each subplot.

of view, value 0.1 day is a good compromise. We considered 3 years from 1 January 2000 to 31 December 2002, in which $\text{SYM-H} < -40$ nT. In each case, we reconstructed E_y vs. SYM-H scatter plots and selected the events, for which a typical pattern (similar to one in Fig. 2c) was recognizable. We omitted those complicated cases, in which the SYM-H index exhibited strong fluctuations due to previous non-quiet magnetospheric conditions before the main phase of geomagnetic storms. The 0.1 day-long time interval in the time shifted solar wind measurements was chosen to be at the beginning of the main phase of a storm. We selected only those events, in which multi-scale fluctuations were present in both B_z and E_y and Eq. (3) was fulfilled at the same time. Following these selection criteria we found 23 events during the time interval selected. Then we compared the standard deviations and anisotropy angles (computed from 0.1 day-long solar wind magnetic field data) with $\min(\text{SYM-H})$ (in Fig. 1f $\min(\text{SYM-H}) \sim -160$ nT). The duration of the main phase of the geomagnetic storms is usually of the same order (\sim hours) of the time lag, which maximizes the linear correlation coefficient between the fluctuations in the solar wind and the D_{st} index.

Figure 3 shows the scatter plots between $\min(\text{SYM-H})$ and standard deviations of magnetic field components obtained from the solar wind. The correlation coefficient (r) and the p-value corresponding to each pair of variables is shown at the top. The p-value or calculated probability is the estimated probability of rejecting the null hypothesis of a study question when that hypothesis is true. There is no correlation between $\text{std}(B_y)$ and $\min(\text{SYM-H})$ index ($r=0.05$) and a weak negative correlation between $\text{std}(B_x)$ ($r=-0.31$),

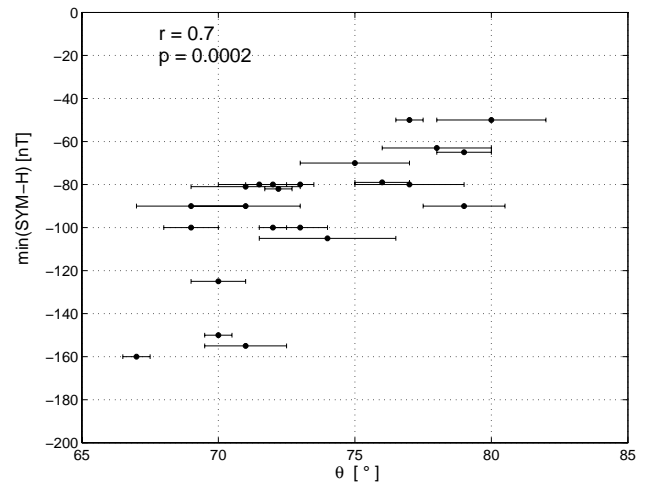


Fig. 4. The time delayed maximum strength of geomagnetic storms, measured by $\min(\text{SYM-H})$, is plotted as a function of the estimated Shebalin anisotropy angles θ . The correlation coefficient (r) and the corresponding p-value are shown on the top.

$\text{std}(B_z)$ ($r=-0.43$) and $\min(\text{SYM-H})$, respectively. If the observed p-value exceeds 0.05, the result is not statistically significant at the 5% level. Therefore, the negative correlation between $\text{std}(B_z)$ and $\min(\text{SYM-H})$ is close to being statistically significant, the other two correlations are not statistically significant. Figure 4 shows positive strong correlation ($r=0.7$) between the anisotropy angle θ and $\min(\text{SYM-H})$. $p=0.0002$ indicates that the correlation is statistically significant. Smaller θ indicate stronger storms (smaller $\min(\text{SYM-H})$) and if $\theta \rightarrow 90^\circ$, turbulence is quasi 2-D and the fluctuations concentrate into the plane perpendicular to the local mean magnetic field.

4 Discussion and conclusions

In this paper we investigated the geoeffectivity of solar wind magnetic turbulence using ACE measurements during duskward electric field driven geomagnetic storms from 2000 to 2002. Two measures of fluctuations computed in sliding windows within a 0.1-day time interval at the beginning of storms were evaluated: the standard deviations of magnetic field components and the Shebalin anisotropy angles. These measures were compared to the minima of SYM-H index (maximum strength of geomagnetic storms), which usually occur a few hours after the beginning of storms. The solar wind measurements were shifted to Earth using the average bulk speed. The approximate value of the time shift was corrected on the basis of visual inspection of the associated patterns in the $E_y - \text{SYM-H}$ plane. Only geomagnetic storms with well-defined Shebalin angles associated with multi-scale fluctuations in the solar wind were selected.

The comparison of standard deviations of magnetic field fluctuation components estimated at the beginning of the main phases of geomagnetic storms with $\min(\text{SYM-H})$ revealed that the correlations are zero or weak. Only $\text{std}(B_z)$ and $\min(\text{SYM-H})$ show statistically significant results at the 5% level. It has already been shown that the correlation between the amplitude of the solar wind turbulence constructed from standard deviations of B_x , B_y , B_z and the D_{st} index improves if a several-hour time lag is introduced between the solar wind and the D_{st} measurements (Borovsky and Funsten, 2003). However, the correlation is approximately two times weaker than the correlation between upstream turbulence and e.g. auroral indices. It is understandable, because various sources (e.g. current at the magnetopause, ring current, tail current, etc.) contribute to the D_{st} (and SYM-H) index and the effective magnetospheric response can be affected by different time delays between the solar wind input and the corresponding magnetospheric driving sources. On the other hand, we selected duskward electric field driven storms, for which magnetic reconnection at the magnetopause and southward B_z are the key factors. A mean southward B_z always exists for a longer time, as it is depicted in Fig. 1a. Under the influence of dynamical solar wind, an antiparallel orientation of interplanetary and magnetospheric magnetic fields might be unstable. The magnetospheric field lines can also change their orientation under the dynamical pressure of the solar wind. Therefore, we can speculate that the fluctuations of B_z can increase the probability for antiparallel field lines, that is the probability of magnetic reconnection at the magnetopause. A weak correlation between $\text{std}(B_z)$ and SYM-H can occur, because of the increase of probability for magnetic reconnection in fluctuating magnetic fields. The correlation is much stronger between the Shebalin anisotropy angle θ and $\min(\text{SYM-H})$ (Fig. 4). The p-value also indicates that the correlation is statistically significant. Stronger storms (smaller $\min(\text{SYM-H})$) are associated with smaller θ . If θ is close to 90° , turbulence is quasi two dimensional and the fluctuations concentrate into the plane perpendicular to the local mean magnetic field. In the physical space the fluctuations are strongly elongated along the magnetic field direction (e.g. Cho et al., 2003). The fluctuations are more isotropic and parallel fluctuations are not negligible if θ decreases (getting closer to 54°). Only some mean southward B_z is present, when the exact orientation of magnetospheric and interplanetary magnetic fields is not known locally and the appearance of stronger parallel component of fluctuations can increase the probability of magnetic reconnection at the magnetopause. It can explain the strong correlation between anisotropy angles θ (estimated in the solar wind) and the SYM-H index.

We note that other measures can be considered for the description of solar wind turbulence, e.g. higher order statistical moments. Such measures can describe different aspects of multi-scale non-Gaussian fluctuations in the solar wind (Jankovičová et al., 2008).

Acknowledgements. This research was supported by the Grant Agency of the Academy of Sciences of the Czech Republic (Grant No. B300420509), the INTAS Foundation (Grant No. 06-1000017-8943) and the Austrian Wissenschaftsfonds under grant No. P20131-N16. We would like to thank for ACE database and the World data center for Geomagnetism, Kyoto, Japan for geomagnetic SYM-H data. We would like to thank very much Steve Saxonberg, Raffaella D'Amicis and Sean Oughton for their comments, which significantly improved our paper.

Edited by: P.-L. Sulem

Reviewed by: R. D'Amicis and S. Oughton

References

- Borovsky, J. E. and Funsten, H. O.: Role of solar wind turbulence in the coupling of the solar wind to the Earth's magnetosphere, *J. Geophys. Res.*, 108(A6), 1246, doi:10.1029/2002JA009601, 2003.
- Bruno, R. and Carbone, V.: The solar wind as a turbulence laboratory, *Living Rev. Solar Phys.*, 4, 1–186, 2005.
- Burlaga, L. F.: Intermittent turbulence in the solar wind, *J. Geophys. Res.*, 96, 5847–5851, 1991.
- Burlaga, L. F. and Forman, M. A.: Large-scale speed fluctuations at 1 AU on scales from 1 hour to 1 year: 1999 and 1995, *J. Geophys. Res.*, 107(A11), 1403, doi:10.1029/2002JA009271, 2002.
- Cho, J., Lazarian, A., and Vishniac, E. T.: MHD turbulence: Scaling laws and astrophysical implications, in: *Turbulence and magnetic fields in astrophysics*, edited by: Falgarone, E. and Passot, T., Springer LNP 614, 56–98, 2003.
- D'Amicis, R., Bruno, R., and Bavassano, B.: Is geomagnetic activity driven by solar wind turbulence?, *Geophys. Res. Lett.*, 34, L05108, doi:10.1029/2006GL028896, 2007.
- Gonzalez, W. D. and Tsurutani, B. T.: Criteria of interplanetary parameters causing intense magnetic storms ($D_{st} < -100$ nT), *Planet. Space Sci.*, 35, 1101–1109, 1987.
- Gonzalez, W. D., Tsurutani, B. T., and de Gonzalez, A. L. C.: Interplanetary origin of geomagnetic storms, *Space Sci. Rev.*, 88, 529–562, 1999.
- Gonzalez, W. D., Tsurutani, B. T., Lepping, R. P., and Schwenn, R.: Interplanetary phenomena associated with very intense geomagnetic storms, *J. Atmosph. Solar Terr. Phys.*, 64, 173–181, 2002.
- Jankovičová, D., Vörös, Z., and Šimkanin, J.: The influence of solar wind turbulence on geomagnetic activity, *Nonlin. Processes Geophys.*, 15, 53–59, 2008, <http://www.nonlin-processes-geophys.net/15/53/2008/>.
- Matthaeus, W. H., Oughton, S., Ghosh, S., and Hossain, M.: Scaling of anisotropy in hydromagnetic turbulence, *Phys. Rev. Lett.*, 81, 2056–2059, 1998.
- McPherron, R. L., Baker, D. N., Bargatze, L. F., Clauer, C. R., and Holzer, R. E.: IMF control of geomagnetic activity, *Adv. Space Res.*, 8, (9)71–(9)86, 1988.
- Oughton, S., Matthaeus, W. H., and Ghosh, S.: Scaling of spectral anisotropy with magnetic field strength in decaying magnetohydrodynamic turbulence, *Phys. Plasmas*, 5(12), 4235–4242, 1998.
- Oughton, S., Matthaeus, W. H., and Ghosh, S.: Anisotropy and energy decay in magnetohydrodynamic turbulence: theory and solar wind observations, in: *Advances in Turbulence VII, Proceed-*

- ings of the Seventh European Turbulence Conference, Saint-Jean Cap Ferrat, France, 30 Jun–3 Jul, edited by: Frisch, U., Kluwer, ISBN 0-7923-5115-0, 1998.
- Sorriso-Valvo, L., Carbone, V., Veltri, P., Consolini, G., and Bruno, R.: Intermittency in the solar wind turbulence through probability distribution functions of fluctuations, *Geophys. Res. Lett.*, 26, 1801–1804, 1999.
- Shebalin, J. V., Matthaeus, W. H., and Montgomery, D. C.: Anisotropy in MHD turbulence due to a mean magnetic field, *J. Plasma Phys.*, 29, 525–547, 1983.
- Vassiliadis, D., Klimas, A. J., Baker, D. N., and Roberts, D. A.: The nonlinearity of models VB(south)-AL coupling, *J. Geophys. Res.*, 101, 19 779–19 788, 1996.
- Vörös, Z., Jankovičová, D., and Kovács, P.: Scaling and singularity characteristics of solar wind and magnetospheric fluctuations, *Nonlin. Processes Geophys.*, 9, 149–162, 2002, <http://www.nonlin-processes-geophys.net/9/149/2002/>.
- Wanliss, J. A., and Showalter, K. M.: High-resolution global storm index: D_{st} versus SYM-H, *J. Geophys. Res.*, 111, A02202, doi:10.1029/2005JA011034, 2006.